CHAPTER 4

Hydrogen in III-V Nitrides

Chris G. Van de Walle and Noble M. Johnson

XEROX PALO ALTO RESEARCH CENTER
3333 COYOTE HILL ROAD
PALO ALTO, CALIFORNIA

I. Introduction

While the technological potential of nitride semiconductors has been appreciated for several decades, current rapid progress in the field resulted from breakthroughs that occurred at the end of the 1980s. One such breakthrough consisted of the achievement of *p*-type doping in GaN. It was found that mere incorporation of acceptor impurities during metal organic chemical vapor deposition (MOCVD) growth was not sufficient; a post-growth processing step, either involving low-energy electron beam irradiation (LEEBI) (Amano *et al.*, 1989) or thermal annealing (Nakamura *et al.*, 1992) was required. It is now understood that hydrogen plays an important role in this process, providing strong motivation for understanding the

ISBN 0-12-752166-6

behavior of hydrogen in the group III-V nitrides. Based on current knowledge about the behavior of hydrogen in other semiconductors, we expect hydrogen to be involved in other important processes as well.

The rest of this Introduction will be devoted to a brief review of the highlights of this knowledge; references to the literature can be found in review volumes by Pankove and Johnson (1991) and by Pearton *et al.* (1992), and in a review paper by Estreicher (1995).

In Section II we will describe what is known from theory and computations about hydrogen in GaN. While many features are similar to the behavior of hydrogen in other semiconductors, a number of important differences occur; the physical reasons for these differences will be discussed. At this stage, experimental knowledge about hydrogen in the nitrides lags the theoretical understanding: the number of physical parameters that have been determined is much lower than for Si or GaAs. A summary of the experimental results obtained to date is given in Section III. Section IV concludes the chapter, with an emphasis on future directions.

1. General Features of Hydrogen in Semiconductors

a. Charge States of Isolated Interstitial Hydrogen

Isolated interstitial hydrogen can assume different charge states in the semiconductor. The impurity introduces a level in the bandgap, and the charge state depends on the occupation of that level. The charge state determines the most favorable location of hydrogen in the semiconductor lattice.

In the positive charge state (H^+, essentially a proton) hydrogen seeks out regions of high electronic charge density. In most covalent semiconductors, the maximum charge density is found at the bond-center (BC) site, and in Si and GaAs H^+ is indeed known to be located at this site. Hydrogen in GaN will turn out to behave differently. This charge state is most favorable in *p*-type material.

In the negative charge state (H^-) hydrogen prefers regions of low electronic charge density. In semiconductors with zinc-blende structure, H^- can be found at the tetrahedral interstitial site; H^- is the preferred charge state in *n*-type material.

The lattice location of neutral hydrogen (H^0), finally, is quite sensitive to the details of the charge density distribution. In all cases that have been theoretically investigated, however, the energy of H^0 is always higher than that of H^+ or H^-, that is, the neutral charge state is never the most

stable state, under equilibrium conditions. This is the defining characteristic of a "negative-U" center. We will see that H in GaN is a negative-U center with a very large magnitude of U.

b. *Diffusion*

Hydrogen, being a small and light impurity, is expected to move quite easily through the perfect lattice. This is indeed true for the positive and neutral charge states. The migration barriers for the negative charge state are usually somewhat higher.

c. *Compensation and Passivation of Shallow Impurities*

Based upon the characteristics of isolated interstitial hydrogen, one can immediately predict that hydrogen will interact with shallow dopants. Hydrogen always counteracts the electrical activity of the dopants. The presence of hydrogen in p-type material leads to formation of H^+, a donor, which compensates acceptors. When H^+ forms a *complex* with the acceptor impurity (to which it is coulombically attracted), we say that the acceptor is *passivated* (*or neutralized*). *Passivation* is characterized by the presence of neutral complexes (which cause little scattering of carriers), whereas *compensation* involves donors and acceptors that are spatially separated (and hence contribute separately to ionized impurity scattering); the difference can be observed in carrier mobilities.

The *binding energy* of hydrogen to the shallow-level is defined as the energy difference between the initial state (a complex) and the final state (hydrogen and the shallow dopant far apart). This binding energy is usually of order 1 eV. The *dissociation energy* is the activation energy required to break up the complex; it is somewhat higher than the binding energy, due to the presence of a barrier in the potential energy surface. Dissociation of the complex usually requires annealing at a temperature of a few hundred degrees Centigrade. Studies of the dissociation kinetics are most reliably performed with the complex situated in an electric field, such as that present in the space charge region of a reverse biased diode; the electric field removes the dissociated hydrogen from the vicinity of the dopant and prevents retrapping. In the absence of an electric field, higher annealing temperatures are required to activate the dopants due to retrapping. It has also been found that minority carriers can enhance the dissociation process.

Just as H^+ passivates acceptors, we expect H^- to passivate donors. The passivation efficiency and activation kinetics depend on the relative stability of the various hydrogen charge states.

d. Interactions with Deep Levels

Hydrogen can of course also interact with impurities or defects that form deep levels in the bandgap. A prime example is the interaction of hydrogen with dangling bonds in amorphous silicon, a process that significantly improves the electronic quality of the material. Hydrogen interacts with native defects, the passivation of vacancies being most extensively studied. Interactions with impurities that introduce deep levels have been observed but have not been studied in great detail. Finally, one expects hydrogen to interact with extended defects as well.

e. Hydrogen Molecules and Molecular Complexes

Theory predicts that H_2 molecules readily form in many semiconductors; the binding energy is somewhat smaller than its value in free space, but still large enough to make interstitial H_2 one of the more favorable configurations hydrogen can assume in the lattice. Experimental observation of these molecules has proven challenging, due mainly to the lack of a dipole moment in the molecule, rendering it difficult to observe with IR absorption spectroscopy. The H_2 molecules seem to form often after H has been released from shallow dopants. We will see in Section III that H_2 molecules are not nearly as favorable in GaN as they are in the other semiconductors.

Another configuration involving two hydrogen atoms is the so-called H_2^* complex, in which a host-atom bond is broken and one hydrogen atom is inserted between the two atoms, in a BC position, while the other hydrogen occupies an antibonding (AB) site. This configuration is somewhat higher in energy than the H_2 molecule, at least in diamond, silicon, and GaAs, but it may play an important role in diffusion as well as in nucleation of larger hydrogen-induced defects.

2. PRESENCE OF HYDROGEN DURING NITRIDE GROWTH AND PROCESSING

Hydrogen can be incorporated in the semiconductor either intentionally or unintentionally. Techniques for intentional hydrogenation are reviewed by Pankove and Johnson (1991). The preferred technique of introducing hydrogen in a controlled fashion is hydrogenation in a remote plasma. Shielding the sample from the plasma prevents introduction of plasma-induced defects. Atomic hydrogen, generated in the plasma, can be introduced in the semiconductor at moderate temperatures, unlike molecular hydrogen, which penetrates only at high temperatures. Isotope studies can be performed by using deuterium (^{2}H); deuterium also lends itself to

detection by secondary ion mass spectroscopy (SIMS), where the presence of hydrogen in the background limits the sensitivity of SIMS to ^1H.

Hydrogen can also be introduced using proton implantation. Implantation always carries the risk of creating damage in the solid; such damage is very difficult to anneal out in a hard material such as GaN. The effects of hydrogen introduced by implantation are therefore often hard to separate from those caused by the implantation damage. Sometimes the implantation damage itself is actually the sought-after effect of proton implantation, for instance for device isolation (Binari *et al.*, 1995).

Unintentional incorporation of hydrogen can occur during a host of processes. First and foremost, MOCVD growth is bound to introduce large concentrations of hydrogen, both from the source gases and from the use of H_2 as a carrier gas. This also applies to hydride vapor phase epitaxy (HVPE). Growth by molecular beam epitaxy (MBE) is often considered to be free of hydrogen; in reality, however, measurable concentrations of hydrogen have been found in MBE-grown samples. Hydrogen is usually the prevailing contaminant in MBE chambers; it can be introduced through water vapor, from sources, and so on. Recently, Yu *et al.* (1996) have intentionally introduced hydrogen during MBE growth of GaN, finding that hydrogen favorably affects growth under Ga-rich conditions. These findings will be discussed in Section III. Finally, post-growth processing of samples can also introduce hydrogen; among the examples are annealing in forming gas and chemomechanical polishing.

II. Theoretical Framework

1. Theoretical Approaches Used for Hydrogen in Nitrides

Most of the theoretical studies carried out for hydrogen in GaN to date are based on density-functional theory in the local-density approximation, using pseudopotentials, a plane-wave basis set, and a supercell geometry (Neugebauer and Van de Walle, 1995a; Bosin *et al.*, 1996; Okamota *et al.*, 1996). Only one study has been based on a different approach, namely, Hartree-Fock based cluster calculations (Estreicher and Maric, 1996). A thorough discussion of these methods has been given by Estreicher (1994, 1995). Here we provide only a brief overview of the techniques.

a. Pseudopotential-Density-Functional Calculations

This computational approach is now regarded as a standard for performing first-principles studies of defects in semiconductors. Density functional theory (DFT) in the local density approximation (LDA) (Hohenberg and

Kohn, 1964; Kohn and Sham, 1965) allows a description of the ground state of the many-body system in terms of a one-electron equation with an effective potential. The total potential consists of an ionic potential due to the atomic cores, a Hartree potential, and a so-called exchange and correlation potential that describes the many-body aspects. This approach has proven very successful for a wide variety of solid-state problems. One shortcoming of the technique is its failure to produce reliable excited-state properties, widely referred to as the "bandgap problem." Many useful results of the calculations depend on ground-state properties and are thus not affected by this shortcoming. In cases where the bandgap enters the calculations either directly or indirectly, judicious inspection of the results still allows extraction of reliable information. Situations where the bandgap error could potentially affect the results will be discussed where appropriate (see Neugebauer and Van de Walle, 1995b).

Most properties of molecules and solids are determined by the valence electrons; the core electrons can usually be removed from the problem by representing the ionic core (i.e., nucleus plus inner shells of electrons) with a pseudopotential. State-of-the-art calculations employ nonlocal norm-conserving pseudopotentials (Hamann *et al.*, 1979) that are generated solely based on atomic calculations and do not include any fitting to experiment.

The case of the nitride semiconductors poses two challenges for the use of pseudopotentials. First, nitrogen is a first-row element characterized by a fairly deep potential, which requires a rather large cutoff in the plane-wave basis set that is commonly used to expand wave functions and potentials in a variational approach. Second, the $3d$ states of Ga (and $4d$ states of In) cannot strictly be considered as core states. Indeed, the energetic position of these states is fairly close to the N $2s$ states, and the interaction between these levels may not adequately be described if the d states are treated as part of the core. Including the d electrons as valence states significantly increases the computational burden, because their wave functions are much more localized than those of the s and p states. Sometimes explicit inclusion of the d states as valence states is the only way to obtain accurate results (Neugebauer and Van de Walle, 1994a). In many cases, however, the effect of the d states can be adequately included by a correction to the exchange and correlation potential, commonly referred to as the "nonlinear core correction" (Louie *et al.*, 1982). Specifically, for the case of the hydrogen impurity in GaN, tests have shown that use of the nonlinear core correction provides a reliable description of the system (Neugebauer and Van de Walle, 1995b).

The last ingredient commonly used in pseudopotential-density-functional

calculations for defects or impurities is the supercell geometry. Ideally, one would like to describe a single isolated impurity in an infinite crystal. In the supercell approach, the impurity is surrounded by a finite number of semiconductor atoms, and this structure is periodically repeated. Maintaining periodicity allows continued use of algorithms such as fast Fourier transforms (FFT). One can also be assured that the band structure of the host crystal is well described (which may not be the case in a cluster approach). For sufficiently large supercells, the properties of a single, isolated impurity can be derived. Convergence tests have indicated that the energetics of impurities and defects are usually well described by using 32-atom supercells. Specific cases, such as description of highly charged states or detailed investigations of wave functions of shallow impurities, may require larger supercells, but at present that is still computationally challenging.

Error bars on the values derived from first-principles calculations depend on the situation. When comparing energies of an impurity in different positions in the lattice, the accuracy is quite high and the error bar is smaller than 0.1 eV. When looking at formation energies, or comparing energies of different charge states, the limitations of density-functional theory may play a role, and the error bar could increase to a few tenths of an electron volt. These error bars are still small enough not to affect any of the qualitative conclusions discussed here.

b. Hartree-Fock Based Cluster Calculations

Hartree-Fock based models are usually based on quantum-chemistry approaches that have been successfully applied to atoms and molecules. The main problem with the technique is the computational demands: *ab initio* Hartree-Fock methods can only be applied to systems with small numbers of atoms, because they require evaluation of a large number of multicenter integrals. Various semiempirical approaches have been developed that either neglect or approximate some of these integrals. The accuracy and reliability of these methods are hard to assess.

In the cluster approach, the crystalline environment is simulated by a cluster of host atoms, typically terminated by hydrogen atoms. The impurity is then embedded in such a cluster. Size–convergence tests should ensure that the cluster is large enough to suppress any spurious interactions with the surface of the cluster, and to provide a reasonable description of the host band structure. The latter is usually challenging, because for cluster sizes that are computationally tractable the confinement of the electronic states will lead to significant modifications of the bulk band structure.

2. ISOLATED INTERSTITIAL HYDROGEN IN GaN

a. Configurations in the Lattice

Comprehensive calculations of the energetics, atomic geometry, and electronic structure for isolated hydrogen in a variety of different interstitial positions in GaN were carried out by Neugebauer and Van de Walle (1995a, 1995b) and by Bosin *et al.* (1996). Both groups used the pseudopotential-density functional approach, and their conclusions are very similar. Some quantitative differences will be discussed where appropriate. Estreicher and Maric (1996) reported preliminary Hartree-Fock based calculations on clusters of zinc-blende–GaN containing 44 host atoms. Their results will also be included in what follows.

Neugebauer and Van de Walle actually mapped out complete total-energy surfaces by placing the hydrogen atom in a variety of positions in the crystal and allowing the host atoms to relax. The resulting energies as a function of hydrogen position form an adiabatic total energy surface, and include information abut diffusion barriers. The calculations of Neugebauer and Van de Walle (1995a, 1995b) were carried out for GaN in the zinc-blende structure; those of Bosin *et al.* (1996) for the wurtzite structure, but only exploring sites with C_{3v} symmetry. As the zinc-blende and wurtzite structures only differ beyond third-nearest neighbors, the differences with respect to atomic and electronic structure of the hydrogen impurity are expected to be small.

Hydrogen in the positive charge state: H^+. In the positive charge state, hydrogen as usual seeks out regions of high electronic charge density; in the GaN crystal, this means positions close to the nitrogen atom. Indeed, the first-principles calculations show that essentially all positions in which the H–N bond length is about 1.02 Å are approximately equal in energy, this bond length being representative of H–N bonds in molecules. This situation is different from more covalent semiconductors such as Si and GaAs; there, the covalent nature of the bonding leads to a significant buildup of charge in the bonds between the atoms. In a more ionic crystal such as GaN this concentration of charge in the bonds is less pronounced, and the charge density is distributed more spherically around the anion. Still, the charge density peaks in the bonds between the atoms, and H^+ would probably still prefer this site, were it not for another effect that counterbalances the energy gained by immersing the proton in a region of high electronic density. This effect is the lattice relaxation that is required to accommodate the H^+ at the BC site. Indeed, the Ga–N bond length of 1.95 Å is too short to allow for insertion of a H atom; the Ga–N bond has

to stretch by more than 40% of the bond length. This relaxation obviously costs energy, and it is particularly costly in a hard material such as GaN. In spite of this high cost, the BC site is still only a few 0.1 eV higher in energy than the AB_N site (antibonding site behind nitrogen atom), where virtually no relaxation is necessary, and which provides the most stable site for H^+. Estreicher and Maric (1996), in their Hartree-Fock based calculations, actually found H^+ to reside at the BC site.

The total energy surface for H^+ (Neugebauer and Van de Walle, 1995a) shows that H^+ can move between equivalent sites in the lattice with a barrier of only 0.7 eV. This rather low value is indicative of a high diffusivity. Indeed, experiments on hydrogen diffusion (to be discussed in Section III) have confirmed this prediction of high mobility for H^+.

Hydrogen in the neutral charge state: H^0. The energy differences between different sites are much smaller for H^0 than they are for H^+, that is, the total energy surface is rather flat (except for regions within 1 Å of the nuclei, where the energy always increases sharply). This behavior is similar to the trend in Si (Van de Walle *et al.*, 1989). Neugebauer and Van de Walle (1995a) find the most stable site to be the antibonding site behind a Ga atom (AB_{Ga}). As the Ga–H bond length is only about 0.1 Å smaller than the Ga–N bond length, the AB_{Ga} site nearly coincides with the position of the tetrahedral interstitial site (T_d^{Ga}) in the zinc-blende structure. Bosin *et al.* find the BC site to have the lowest energy; a possible explanation for the difference will be given in what follows. Estreicher and Maric (1996) reported that for H^0 the BC site is nearly degenerate with the T_d^{Ga} site.

Hydrogen in the negative charge state: H^-. All calculations find that the most stable site for H^- is at the AB_{Ga} site (very close to T_d^{Ga}, as already discussed). The charge density of the GaN crystal has a global minimum at this site, rendering it favorable for incorporation of a negatively charged impurity. Other sites in the crystal are much higher in energy. Consequently, the energy barrier for H^- to move between equivalent sites is quite high; the total energy surface (Neugebauer and Van de Walle, 1995a) yields a migration barrier of 3.4 eV, a value high enough to render H^- essentially immobile.

b. *Relative Stability of Different Charge States and "Negative-U" Character*

The first-principles calculations also allow a comparison of the energy of hydrogen in different charge states. These energy differences necessarily depend on the position of the Fermi level; for instance, in order to convert

H^0 into H^+, an electron has to be removed from H^0, and the energy of this electron has to be taken into account in the comparison of energies. In a thermodynamic context the electrons are placed in the reservoir of electrons, with an energy corresponding to the Fermi energy (E_F). If the Fermi level is high in the gap, it will cost more energy to place an electron there, and consequently the energy difference between H^+ and H^0 will increase. The energy of the neutral species is, of course, independent of the Fermi energy. The *formation energy* of interstitial H^0 is defined as the energy difference between a free H atom (in vacuum) and H^0 at its stable site inside GaN. In thermodynamic equilibrium, the formation energy determines the concentration c of an impurity at temperature T through the following expression:

$$c = N_{\text{sites}} \exp[-E^f/k_B T] \tag{1}$$

where N_{sites} is the number of sites on which the defect can be incorporated, k_B the Boltzmann constant, and E^f the formation energy. The formation energies of interstitial hydrogen in various charge states in GaN are depicted in Fig. 1. Bosin *et al.* (1996) produced a similar figure, but with some

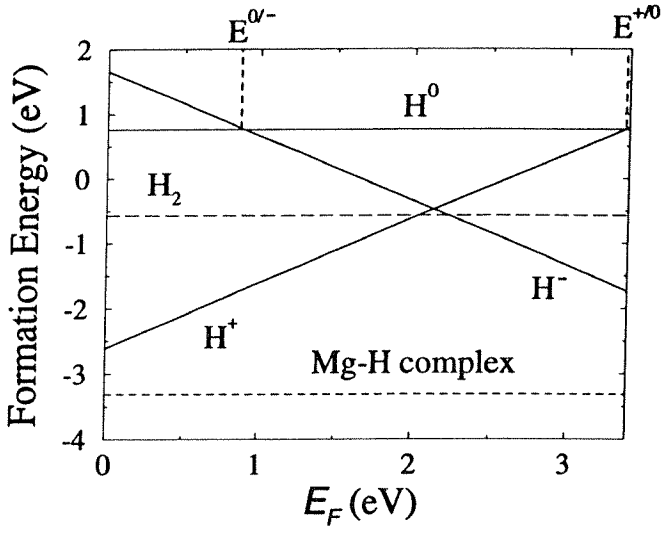

FIG. 1. Formation energies as a function of Fermi level for H^+, H^0, and H^- (solid lines), for a H_2 molecule (dashed line), and for a Mg-H complex (short-dashed line) in GaN. $E_F = 0$ corresponds to the top of the valence band. The formation energy is referenced to the energy of a free H atom. (Reprinted with permission from Neugebauer and Van de Walle, 1995a.)

quantitative differences. Most of these differences can be traced back to the difference in bandgaps that occur in the computational approaches. The small value of the gap in the calculations by Bosin *et al.* probably causes them to occupy states (for the case of H^0 and H^-) that are not H-induced impurity levels, but conduction-band states. This incorrect level occupation then affects the formation energies, and may also be responsible for the different conclusions regarding the stable position of the H^0 species. We now discuss several conclusions that can be drawn from Fig. 1.

Incorporation in the lattice and solubility. Figure 1 shows that the formation energy of H^+ can be significantly lower than that of H^-. According to Eq. (1), lower formation energies translate into higher concentrations that can be incorporated in the solid. We therefore see that conditions favoring formation of H^+ will lead to higher levels of hydrogen incorporation. Figure 1 shows that H^+ has a lower formation energy in *p*-type material (low values of E_F), while H^- is lower in energy in *n*-type GaN (high values of E_F). We therefore conclude that hydrogen is more likely to incorporate in *p*-type GaN than in *n*-type material. This prediction has been confirmed in a number of experiments, to be discussed in Section III. Values of E_F below ~ 2.1 eV favor incorporation of H^+; for E_F higher in the gap, H^- is more stable. Note that H^0 is not the lowest-energy species for *any* position of the Fermi level; this is characteristic of a "negative-U" center, to be discussed in the next section.

Transition levels and negative-U. Our discussion so far indicates that hydrogen is an amphoteric impurity, that is, it behaves as both a donor and an acceptor. The position of E_F for which the formation energies of H^+ and H^0 are equal is, by definition, the donor level of an impurity. Similarly, the E_F value for which the formation energies of H^0 and H^- coincide determines the acceptor level. These acceptor and donor levels can be determined from Fig. 1, the most obvious conclusion being that the donor level is located *above* the acceptor level, by a value of 2.4 eV. This is a rather unusual situation for impurities in semiconductors; more commonly, Coulomb repulsion (expressed by the parameter U) makes it more difficult to add additional electrons to an impurity and, therefore, the acceptor level (the $0/-$ transition) is expected to lie above the donor level ($+/0$) ("positive-U"). The energy difference between the acceptor and the donor level is negative here, characteristic of a "negative-U" center. This behavior can occur because hydrogen assumes different configurations in the lattice as the charge state changes.

The value of U predicted here, -2.4 eV, is larger in magnitude than any value predicted or measured for any impurity in any semiconductor! While

smaller in magnitude, negative-U behavior is also observed for hydrogen in other semiconductors: $U = -0.4$ eV has been calculated (Van de Walle *et al.*, 1989) and measured (Johnson *et al.*, 1994) for Si, and in GaAs, a value of -0.7 eV has been calculated (Pavesi and Giannozzi, 1992). The tendency of hydrogen to form negative-U centers, and the large magnitude of U in GaN can be understood in the context of a simple model for the interaction between H and the semiconductor (Neugebauer and Van de Walle, 1995a).

3. HYDROGEN MOLECULES

Neugebauer and Van de Walle (1995a) have studied the incorporation of H_2 molecules in the GaN lattice. Various interstitial positions were investigated, all yielding about the same formation energy, which is shown in Fig. 1. It is clear that H_2 is unstable with respect to dissociation into monatomic hydrogen. This is a distinct property of GaN, and very different from the case of Si and GaAs. The low stability of H_2 can be explained by the small lattice constant of GaN, which leaves little room for incorporation of a molecule in interstitial positions. Neugebauer and Van de Walle (unpublished) also studied H_2^* complexes (see Section I.1.e), and found them to be higher in energy than H_2 molecules.

4. INTERACTION OF HYDROGEN WITH SHALLOW IMPURITIES

Knowledge of the behavior of isolated interstitial hydrogen already provides major clues to the interaction of hydrogen with shallow acceptors. Incorporation of acceptor impurities renders the material p-type, and we have seen that hydrogen prefers the positive charge state (H^+) in p-type GaN. Hydrogen therefore acts as a donor, counteracting the intended doping of the material. When hydrogen is spatially separated from the acceptor, *compensation* occurs: an electron is transferred from the hydrogen to the acceptor, eliminating a hole that could otherwise have been contributed by the acceptor. Because H^+ is coulombically attracted to negatively charged acceptors, complex formation is possible; this situation is referred to as *passivation*. The difference with compensation can be observed, for example, in carrier mobilities: passivation leads to neutral complexes that cause less scattering than isolated ionized donor and acceptor impurities. Another signature of complex formation is the occurrence of vibrational modes characteristic of the complex. Whether or not the hydrogen forms a complex with the acceptor depends on the binding energy of the complex, and on the temperature.

a. *The Mg-H Complex*

Magnesium is the most commonly used acceptor in GaN; investigations of hydrogen interactions with acceptors have therefore focused on Mg. Bosin *et al.* (1996) also studied the interaction of hydrogen with other acceptor impurities, in particular, Be_{Ga}, C_N, Ca_{Ga}, and Zn_{Ga}. However, the authors pointed out that their results were preliminary due to the limited size of the supercell (16 atoms) and an incomplete investigation of all possible sites.

Several groups (Neugebauer and Van de Walle, 1995a; Bosin *et al.*, 1996; Okamoto *et al.*, 1996) have performed detailed calculations of the interaction between hydrogen and a Mg acceptor. As in the case of isolated H^+, the sites around the N atom are energetically preferred, with the AB_N site apparently winning out over the BC site. Okamoto *et al.* find the BC site to be slightly more favorable than the AB site, but only by 0.1 eV. This small quantitative difference may be due to their use of a smaller wurtzite supercell (16 atoms, as opposed to 32 atoms used by the other groups). The binding energy of the Mg-H complex is 0.7 eV (see also Fig. 1) (Neugebauer and Van de Walle 1995a, 1996a). The binding in the Mg-H complex is clearly dominated by hydrogen interacting with a nitrogen atom, and this is reflected in the vibrational frequency of the stretch mode, which is representative of N—H bonds (such as in NH_3). A comparison of results from the various calculations is presented in Table I. While the qualitative

TABLE I

RESULTS OF COMPUTATIONAL STUDIES OF Mg-H COMPLEXES IN GaN BY VARIOUS GROUPS

Reference	H Site	Structure	Symmetry	ΔE (eV)	Frequency (cm^{-1})
Neugebauer and	AB	zb	C_{3v}	0.0	—
Van de Walle (1995a)	BC	zb	C_{3v}	0.3	3360
Bosin *et al.* (1996)	AB	w	C_s	0.00	2939
	AB	w	C_{3v}	1.13	3069
	BC	w	C_s	0.62	3917
	BC	w	C_{3v}	0.32	3611
Okamoto *et al.* (1996)	BC	w	C_s	0.0	3450
	BC	w	C_{3v}	0.0	3490
	AB	w	?	0.1	—

The H site is either AB, the antibonding site next to a N neighbor of the Mg atom, or BC, the bond center site; "w" stands for wurtzite, "zb" for zinc blende; for the wurtzite structure the complex can be either oriented along the *c*-axis (C_{3v} symmetry), or in the other bonds (C_s symmetry); ΔE is the energy difference with the lowest-energy configuration within each calculation; the frequency of the vibrational stretch mode is given.

conclusions are very similar, some quantitative differences occur. The value calculated by Neugebauer and Van de Walle (1995a) is 3360 cm^{-1}, which is somewhat larger than the experimental result (3125 cm^{-1}, see Section III.5). It should be kept in mind that the calculated value does not include anharmonic effects, which are sizable in the case of N—H vibrations; in NH_3 the anharmonicity lowers the frequency by 170 cm^{-1} (Johnson *et al.*, 1993). Experimental results for vibrations of the Mg-H complex will be presented in Section III.

The interaction of hydrogen with Mg acceptors nicely explains the necessity of an activation procedure when Mg-doped GaN is grown by MOCVD. The MOCVD process allows ready incorporation of hydrogen in the *p*-type layer. During cooldown this hydrogen forms complexes with the Mg acceptors, eliminating the electrical activity. In order to activate the Mg, the complexes have to be dissociated and hydrogen neutralized or removed from the *p*-type layer.

Neugebauer and Van de Walle (1995a) estimated this dissociation barrier of the Mg—H complex to be 1.5 eV or slightly higher. This value should allow dissociation of the complex at temperatures of a few hundred degrees Centigrade. Experimentally, however, temperatures exceeding 600 °C have been found necessary to activate Mg-doped MOCVD-growth GaN. This indicates that the activation process does not merely consist of dissociating Mg-H complexes. When hydrogen leaves the Mg acceptor, it still behaves as a donor, and therefore can still compensate the acceptor as long as it remains in the *p*-type layer. The hydrogen therefore has to be removed from the *p*-type layer (e.g., into the substrate or through the surface); alternatively, the hydrogen can be neutralized, for example, by binding to extended defects. The process is schematically illustrated in Fig. 2. Formation of H_2 molecules, which is common after acceptor passivation in other semiconductors, is not possible in GaN because of the high formation energy of H_2 (see Section II.3).

b. Role of Hydrogen in Doping of GaN

n-type GaN. As discussed in Section II.2.b, the solubility of hydrogen in *n*-type GaN is quite low, and hence hydrogen will have little or no effect on *n*-type doping. *If* hydrogen were present in *n*-type GaN, it could bind to Si donors with essentially the same binding energy (0.7 eV) as calculated for Mg-H complexes (Neugebauer and Van de Walle, 1996a); however, due to the low solubility of H in *n*-type GaN the hydrogen concentration will be very small. This is fortunate, because the high diffusion barrier of H^- in *n*-type GaN would prevent hydrogen from being removed from the material. This high diffusion barrier is also responsible for the fact that hydrogenation

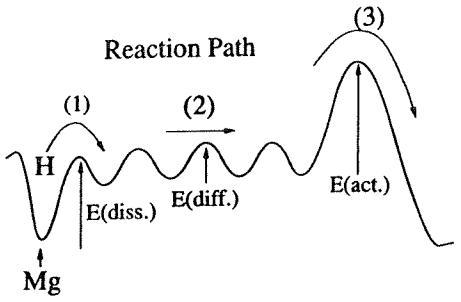

FIG. 2. Schematic illustration of the reaction path and energy barriers for the activation of Mg acceptors in GaN. At low temperatures hydrogen forms a neutral complex with the Mg acceptor. With increasing temperature the Mg-H complex dissociates (1), and the positively charged H can then easily migrate through the crystal (2). Further increase in the temperature allows the hydrogen to overcome an additional activation barrier (3), corresponding to removal from the *p*-type layer or neutralization at extended defects, clusters, and so on. (Reprinted with permission from Neugebauer and Van de Walle, 1996b.)

(exposure to atomic hydrogen) has no discernible effect on *n*-type GaN (Götz *et al.*, 1995).

p-type GaN. In order to appreciate how hydrogen affects the concentrations of acceptor impurities and native defects in the system, we need to go back to the concept of formation energy that was introduced in Section II.2.b, and define formation energies for other species. For all of these species, Eq. (1) will apply, providing the link between formation energy and concentration. The formation energy of a Mg acceptor in GaN depends on various parameters. In addition to the dependence on Fermi level that occurs for a charged species (as discussed in Section II.2.b), the formation energy also depends on the relative abundances of Mg, Ga, and N. In thermodynamic equilibrium these abundances can be described by the chemical potentials μ_{Mg}, μ_{Ga}, and μ_N. A first-principles calculation can provide a value $E_{tot}(GaN{:}Mg_{Ga}^{-})$ for the energy of a GaN supercell in which one Ga atom has been replaced by a Mg atom. The expression for the formation energy then takes into account that a Ga atom had to be removed (and placed in the appropriate reservoir, with energy μ_{Ga}), and that a Mg atom has been brought in from a reservoir with energy μ_{Mg}

$$E^f(GaN{:}Mg_{Ga}^{-}) = E_{tot}(GaN{:}Mg_{Ga}^{-}) - E_{tot}(GaN\text{-bulk}) - \mu_{Mg} + \mu_{Ga} - E_F \qquad (2)$$

Similar expressions apply to the hydrogen impurity, and to any defects that may be present in the system. Extensive investigations of native defects in

GaN (Neugebauer and Van de Walle, 1994b; Boguslawski *et al.*, 1995) have indicated that self-interstitials and antisites are high-energy defects that are unlikely to occur in GaN; we can therefore focus on vacancies.

The chemical potentials are variables, reflecting the variety of conditions that can occur during growth. To facilitate the discussion, however, we focus on a specific set of conditions, namely, Ga-rich growth ($\mu_{Ga} = \mu_{Ga\text{-bulk}}$), and Mg incorporation limited by the formation of Mg_3N_2, which determines the solubility limit of Mg. The formation energy then becomes solely a function of the Fermi energy, as shown in Fig. 3. Results for other growth conditions can easily be derived by changing the chemical potential values.

Figure 3 summarizes the results of Neugebauer and Van de Walle (1996b) for magnesium and native defects in *p*-type GaN, in the absence of hydrogen. The nitrogen vacancy V_N is the dominant defect under *p*-type conditions [note that V_N has a *high* formation energy in *n*-type GaN, and hence is not the cause of *n*-type conductivity in as-grown GaN (Neugebauer and Van de Walle, 1994b; Van de Walle and Neugebauer, 1997)]. The transition between Mg^0 and Mg^- indicates the position of the Mg acceptor level, close to the experimental value of 0.16 eV (Akasaki *et al.*, 1991). These formation energies can be used to calculate equilibrium concentrations, using Eq. (1) and taking charge neutrality into account (for details of this procedure, see Laks *et al.*, 1991 and Van de Walle *et al.*, 1993).

When no hydrogen is present in the system (see Fig. 3) the nitrogen vacancy is the dominant compensating defect, and due to charge neutrality the Fermi level will be located near the point where the formation energies

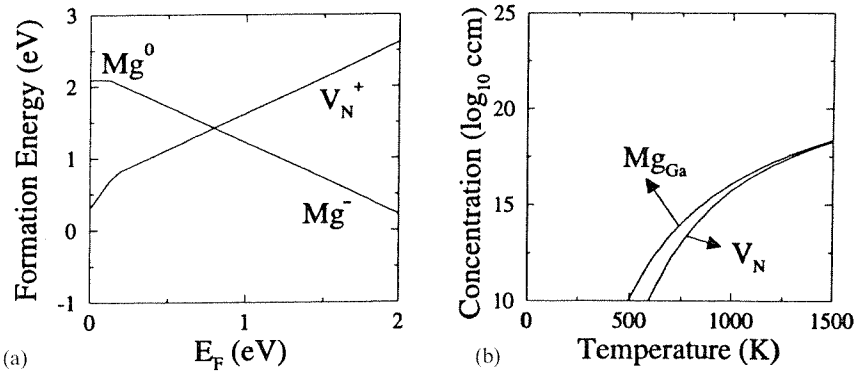

FIG. 3. (a) Formation energies as a function of Fermi level for the Mg acceptor (Mg_{Ga}) and the nitrogen vacancy (V_N). (b) Equilibrium concentrations of these defects and impurities as a function of temperature, in the absence of hydrogen. (Reprinted with permission from Neugebauer and Van de Walle, 1996b.)

of V_N^+ and Mg_{Ga}^- are equal. Significant compensation by nitrogen vacancies would therefore occur; this is a concern, for example, for MBE growth, where little or no hydrogen is present. However, MBE growth is performed at much lower temperatures than MOCVD, and therefore the assumption of thermodynamic equilibrium, which is implicit in Fig. 3(b), is likely not fulfilled. Formation of nitrogen vacancies may therefore be suppressed in MBE.

Hydrogen is highly abundant in many of the high-temperature growth techniques such as MOCVD or HVPE. Therefore, we also consider growth under H-rich conditions (determined by the hydrogen chemical potential being set equal to the energy of free H_2). Figure 4(a) shows that the formation energy of hydrogen is lower than that of the nitrogen vacancy; as a consequence, the formation of nitrogen vacancies is suppressed, and hydrogen becomes the dominant compensating center, as can be seen in Fig. 4(b). We also note that the Mg concentration is increased with respect to the hydrogen-free case. This can be understood by inspection of the formation energies: as the formation energy of hydrogen is lower than that of V_N, the Fermi level equilibration point is moved higher in the gap, leading to a lower formation energy and hence higher concentration of Mg. Incorporation of hydrogen is therefore beneficial in two respects: suppression of native defects and enhancement of the acceptor concentration.

Incorporation of hydrogen of course has the downside that complete compensation of the acceptors occurs. Note that hydrogen is found to be present in the acceptor-doped material *at the growth temperature*; that is,

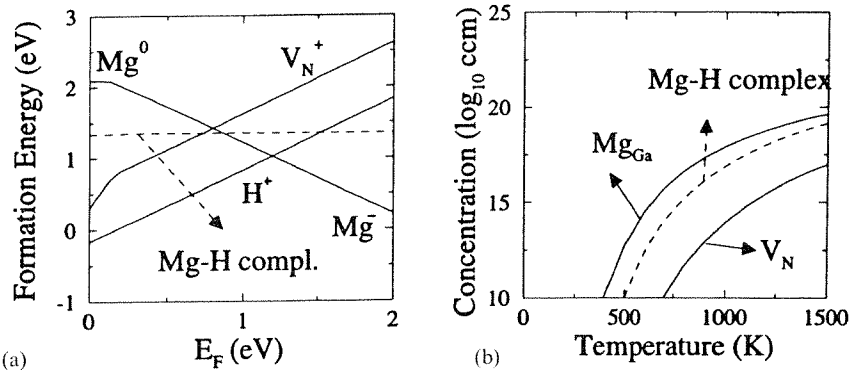

FIG. 4. (a) Formation energies as a function of Fermi level for the Mg acceptor (Mg_{Ga}), the nitrogen vacancy (V_N), and interstitial hydrogen in *p*-type GaN. The formation energy of the Mg-H complex is also shown. (b) Equilibrium concentrations of these defects and impurities as a function of temperature, for the H-rich limit. (Reprinted with permission from Neugebauer and Van de Walle, 1996b.)

hydrogen incorporation occurs during growth, and not merely from the NH_3 ambient during cooldown after growth. This incorporation process may differ from that in some other III-V compounds, where incorporation of hydrogen results mainly from indiffusion during the cooldown process. Hydrogen is thus already present in *p*-type GaN during growth, although not in the form of Mg—H complexes: at the high temperatures used during growth, these complexes are essentially dissociated. After growth, during the cooldown process, the highly mobile H^+ is coulombically attracted to Mg^- acceptors, and eventually forms Mg—H complexes. These complexes can be dissociated, and hydrogen removed from the *p*-type layer, during a post-growth activation process as already described.

General criteria for hydrogen to enhance doping. Van Vechten *et al.* (1992) pointed out that incorporation of hydrogen enables *p*-type doping by suppressing compensation by native defects. They went on to propose the incorporation (and subsequent removal) of hydrogen as a general method for improving *p*-type as well as *n*-type doping of wide-bandgap semiconductors. This model highlights the important role of hydrogen, but leaves various issues unexplained, such as the lack of hydrogen incorporation in *n*-type GaN, and the success of *p*-type doping (without post-growth treatments) in MBE. These issues have now been addressed, as has been described herein. More importantly, the incorporation of a compensating donor should not be considered as a universal solution to doping problems in semiconductors. Indeed, the investigation of H in *p*-type GaN allows us to derive the following general conditions that must be fulfilled for hydrogen (or any other compensating impurity) to improve doping:

(i) Hydrogen must be the dominant compensating defect (i.e., its formation energy must be lower than that of all native defects, and comparable to that of the dopant impurity).

(ii) The activation barriers to dissociate the H-impurity complex and to remove or neutralize H must be lower than the activation energies for native-defect formation, or the diffusion barrier of the impurity.

(iii) The dissociated hydrogen atom must be highly diffusive.

Whether or not these conditions are realized depends on the specific situation (semiconductor, dopant impurity, growth conditions). All of the conditions are met in *p*-type GaN, judging from the success of post-growth annealing. Failure to meet condition (ii) is the likely cause of the difficulties in obtaining *p*-type activity in MOCVD-grown nitrogen-doped ZnSe. Indeed, the N—H bond is very strong and would require high temperatures

for dissociation; these temperatures exceed those at which the structural quality of the ZnSe crystal can be maintained.

III. Experimental Observations

1. INTENTIONAL HYDROGENATION AND DIFFUSION IN GaN

There is now a general consensus among experimentalists that at least in MOCVD-grown material the ability to diffuse hydrogen into GaN at moderate temperatures depends strongly on the electrical conductivity type. This is illustrated in Fig. 5 with results for specimens of *n*-type vs *p*-type GaN that were exposed to monatomic deuterium at specified temperatures for one hour in a remote microwave plasma (Götz *et al.*, 1995). The *p*-type material was Mg doped with a hole concentration of $8 \times 10^{17}\,\mathrm{cm}^{-3}$ at room temperature, and the *n*-type material was Si doped with an electron

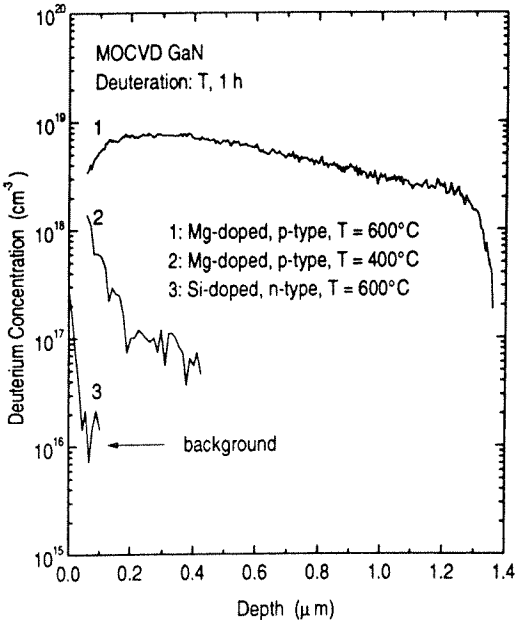

FIG. 5. Deuterium concentration vs depth below the sample surface measured with SIMS. Depth profiles were recorded for *p*-type, Mg-doped GaN after remote plasma deuteration at 600 °C (Curve 1), after deuteration at 400 °C (Curve 2) and for *n*-type, Si-doped GaN after deuteration at 600 °C (Curve 3). The deuterium background level of the SIMS measurement is $\sim 10^{16}\,\mathrm{cm}^{-3}$, as indicated by the arrow. (Reprinted with permission from Götz *et al.*, 1995.)

concentration of $2 \times 10^{17}\,\mathrm{cm}^{-3}$ at room temperature. Both specimens were ~ 1-μm thick, and the Mg-doped specimen was thermally activated prior to hydrogenation. The figure shows depth profiles of deuterium that were obtained with SIMS. Exposure to monatomic deuterium at 600 °C leads to a substantial incorporation of deuterium in the *p*-type material and a negligible amount, beyond the immediate surface, in *n*-type GaN. Even a hydrogenation at 400 °C introduces more deuterium (e.g., volume concentration at any given depth or total depth integrated deuterium) into *p*-type material than is introduced by the 600 °C hydrogenation in the *n*-type material. The experimental results in Fig. 5 indicate that hydrogen readily diffuses and incorporates in *p*-type GaN at temperatures $\geqslant 600$ °C but not in *n*-type GaN. These results are fully consistent with the total energy calculations of the properties of monatomic hydrogen in GaN, as summarized in Section II.2.

Hydrogen diffusion in GaN has been the focus of several studies in recent years. Pearton *et al.* (1996c, 1996d) noted that hydrogen is easily incorporated in GaN during many different process steps, including boiling in water, wet chemical etching, dielectric deposition using SiH_4, or dry etching. These authors reported an effective diffusivity of $> 10^{-11}\,\mathrm{cm}^2\,\mathrm{s}^{-1}$ at 170 °C. Wilson *et al.* (1995) used SIMS to observe outdiffusion of deuterium from plasma-treated or implanted GaN, AlN, and InN. And hydrogen redistribution during anneal was reported by Zavada *et al.* (1994). A few early studies report penetration of hydrogen into *n*-type GaN [e.g., Pearton *et al.* (1996c, 1996d)]. One possible explanation may be that although hydrogen does not incorporate in bulk *n*-type GaN, it can penetrate heavily defected regions by diffusion through grain boundaries or along extended defects. Therefore, *n*-type samples with high densities of extended defects may exhibit effects after hydrogenation.

2. Effects of Hydrogen During Growth/Hydrogen on GaN Surfaces

Sung *et al.* (1996) reported surface studies of *n*-type GaN $\{000\text{-}1\}$-(1×1) surfaces grown by MOCVD, using time-of-flight scattering and recoiling spectrometry, low-energy electron diffraction, and thermal decomposition mass spectrometry. Elastic recoil detection was used to determine the bulk hydrogen concentration. Apart from various conclusions about the surface structure, they found that hydrogen atoms were bound to the outermost layer of N atoms, protruding outward from the surface with a coverage of three-fourths monolayer. Sung *et al.* proposed an explanation for this coverage in terms of autocompensation of the (1×1) structure. They also

suggested that the presence of hydrogen during GaN growth is an important factor in the growth of material with high crystalline quality: H atoms can maintain sp^3 hybridization of the evolving surface, resulting in less ionic character. A high concentration of hydrogen was also found below the surface, within a depth of 5–10 monolayers from the surface.

Yu *et al.* (1996) investigated the effect of intentional introduction of atomic hydrogen during MBE growth of GaN. An RF plasma source was used for nitrogen, and atomic hydrogen was produced with a thermal cracker. The authors found that in the absence of hydrogen high-quality growth was obtained at 730 °C under Ga-rich conditions. It was found that the presence of atomic hydrogen increased the growth rate by as much as a factor of two. It was suggested that hydrogen increases the effective surface concentration of nitrogen, but the issue requires further investigation.

Chiang *et al.* (1995) studied H_2 desorption and NH_3 adsorption on polycrystalline GaN surfaces with time-of-flight detection of recoiled H^+ and D^+ ions. They found that hydrogen is released from Ga sites at temperatures between 250 and 450 °C. Some N—H species decompose at 500 °C, and hydrogen eventually all desorbs at 600 °C. The authors therefore concluded that during CVD growth of GaN at temperatures above 800 °C, the liberation of surface hydrides can be ruled out as the rate-limiting step. They also showed that hydrogen is mobile on the surface at roughly 250–500 °C, and desorbs in a recombinative fashion. Chiang *et al.* (1995) also observed that H/D exchange can occur rapidly during NH_3 exposure, even at room temperature.

3. PASSIVATION AND ACTIVATION OF Mg ACCEPTORS

The crucial role played by hydrogen in *p*-type GaN was established by Nakamura *et al.* (1992). They showed that MOCVD-grown Mg-doped films, which are highly resistive after growth, become *p*-type conductive after thermal annealing in an N_2 ambient. Earlier, Amano *et al.* (1989) had demonstrated that the activation can also be achieved by low-energy electron-beam irradiation (LEEBI). Nakamura *et al.* then annealed their samples in an NH_3 ambient at 600 °C, and found that the resistivity increased significantly. They concluded that atomic hydrogen produced by NH_3 dissociation was responsible for the passivation of acceptors. The correlation between hydrogen and magnesium concentrations was further investigated by Ohba and Hatano (1994).

The precise mechanism by which LEEBI treatment (Amano *et al.*, 1989) activates acceptors is still controversial. The irradiation process can generate electron-hole pairs. These pairs could either directly provide the energy for

releasing hydrogen from the acceptor; or the presence of minority carriers could lower the dissociation barrier. Alternatively, the irradiation process may cause local heating that effectively leads to thermal dissociation. Experiments by Li and Coleman (1996) monitored the LEEBI process with cathodoluminescence spectroscopy. The fact that the LEEBI process remained effective down to liquid helium temperature was interpreted as evidence for an athermal mechanism.

The influence of minority-carrier injection on the activation process was investigated by Pearton *et al.* (1996a). They found that acceptor activation takes place at a temperature as low as 175 °C under minority-carrier injection (accomplished by forward bias of a *p-n* junction). Conventional annealing under zero-bias conditions does not produce Mg-H dissociation until temperatures are above 450 °C. On the basis of these results the authors suggested that minority-carrier-enhanced dissociation of Mg—H complexes is the mechanism for activation during LEEBI treatment.

While Nakamura *et al.* (1992) introduced hydrogen through dissociation of NH_3, Götz *et al.* (1995) used remote plasma hydrogenation, as described in Section III.1. Götz *et al.* (1996a, 1997) went on to investigate the activation kinetics of Mg acceptors. They annealed Mg-doped samples grown by MOCVD incrementally for 5 min at temperatures ranging from 500 to 850 °C. Figure 6(a) demonstrates the resistivity measured as a function of temperature in the as-grown sample and after each annealing step. The resistivity decreases significantly after the 600 °C annealing step and reaches a value of about 3 Ω-cm at 300 K after annealing at 850 °C. In samples annealed above 700 °C the saturation of the resistivity for measurement temperatures below 200 K is due to hole conduction in an acceptor impurity band. Reliable Hall measurements were possible in samples annealed at temperatures of 600 °C and higher; the resulting hole concentrations are depicted in Fig. 6(b). The data for the anneal at 600 °C reveal acceptor activation over the entire measurement range, whereas the data for the anneals above 700 °C reveal ionization of a shallow acceptor only for temperatures above 200 K, with impurity-band conduction at lower temperatures. Fitting of the Hall-effect data indicates the presence of donor compensation, at a level of about $3 \times 10^{18}\,\mathrm{cm}^{-3}$.

These results are consistent with the picture of Mg—H complexes being present in as-grown, Mg-doped GaN. Hydrogen is incorporated during growth, and Mg—H complexes are formed during cooldown. After growth only a fraction of Mg atoms act as acceptors and the material is semi-insulating. The absence of impurity-band conduction after the 600 °C anneal and its appearance after the 700 °C anneal clearly indicate that the activation of Mg acceptors is due to the generation of Mg-related acceptor states in the bandgap of GaN, and, therefore, strongly supports the existence of Mg—H complexes in the as-grown material.

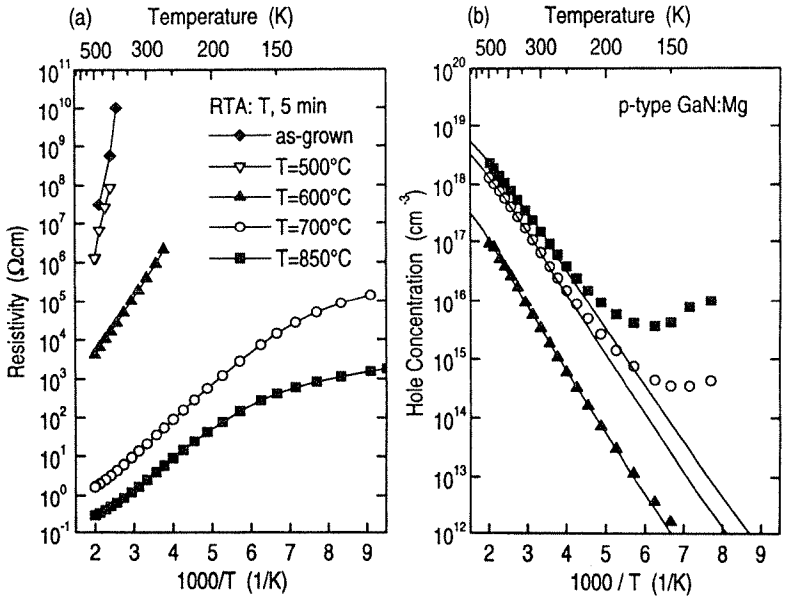

FIG. 6. (a) Resistivity and (b) hole concentration of a Mg-doped GaN sample as a function of reciprocal temperature. The resistivities (a) are shown for as-grown material and after annealing for 5 min at incremental temperatures T. The hole concentrations (b) are shown after acceptor activation at incremental temperatures T. The solid lines (b) represent calculated hole concentrations. (Reprinted with permission from Götz and Johnson, 1997.)

We note that Pearton *et al.* (1996d) reported an activation energy for dopant activation of order 2.5 eV in bulk samples, where hydrogen retrapping is expected to be significant. Pearton *et al.* (1996b) also reported that the apparent thermal stability of hydrogen-passivated Mg acceptors depends on the ambient employed during annealing: an H_2 ambient leads to a reactivation temperature approximately 150 °C higher than N_2. The authors attributed this to indiffusion of hydrogen from the H_2 ambients, causing a competition between passivation and reactivation. They also concluded that the hydrogen does not leave the sample after activation of Mg acceptors, but accumulates in regions of high defect density (in their case, the InGaN layer in a GaN/InGaN double heterostructure).

4. PASSIVATION OF OTHER ACCEPTOR DOPANTS

Hydrogen passivation of Ca acceptors in GaN was reported by Lee *et al.* (1996). The Ca acceptors were introduced by implantation of Ca^+ or Ca^+ with coimplantation of P^+. Exposure to a hydrogen plasma at 250 °C led to

a reduction in sheet carrier density of approximately an order of magnitude. The passivation could be reversed by annealing at 400 to 500 °C under N_2 ambient. The authors concluded that hydrogen passivation of acceptor dopants is a ubiquitous phenomenon, as it is in other semiconductors. Passivation of carbon acceptors was also reported by Pearton *et al.* (1996d).

5. LOCAL VIBRATIONAL MODES OF Mg—H COMPLEX IN GaN

Determination of the local vibrational modes (LVM) of the Mg—H complex in GaN provides satisfying confirmation of the significance of hydrogen in GaN and useful information, when compared with theory, on the structure of the complex. Currently, the stretch frequency is in fact the only reliably established physical parameter available from experiment for the Mg—H complex in GaN.

To provide convincing evidence in support of their spectroscopic identification Götz *et al.* (1996b) performed Fourier-transform infrared absorption spectroscopy on three differently treated specimens of Mg-doped GaN grown by MOCVD: the first specimen was as grown and electrically semi-insulating; the second specimen received a thermal anneal and displayed *p*-type conductivity; the third sample was exposed to monatomic deuterium at 600 °C for 2 hr, which increased the resistivity of the material. The infrared absorption spectra are shown in Fig. 7. The as-grown sample displays an LVM at 3125 cm^{-1}. After thermal activation of the Mg, the intensity of this absorption line is reduced. After deuteration (3), a new absorption line appears at 2321 cm^{-1}, which disappears after a thermal activation treatment (not shown in the figure). The isotopic shift clearly establishes the presence of hydrogen in the complex.

The spectroscopic evidence simultaneously establishes that hydrogen forms a complex with a shallow acceptor and that the acceptor activation process is due to the dissociation of Mg—H complexes. The LVM at 3125 cm^{-1} appears only in Mg-doped GaN, and the isotopic shift is in excellent agreement with that observed for H-related LVMs in other semiconductors (Stavola and Pearton, 1991; Chevallier *et al.*, 1991). Further, the decrease in the intensity of the LVM upon post-growth activation of the *p*-type conductivity is consistent with thermal dissociation of Mg—H complexes. Finally, the assignment of the LVM to the stretch mode of the Mg—H complex is in good agreement with the calculated H-stretch frequency (see Section II.4.a), which establishes that the Mg—H complex contains a strong N—H bond.

In light of the conclusive assignment produced by Götz *et al.* (1996b), we note that the local vibrational modes around 2200 cm^{-1} observed by Brandt

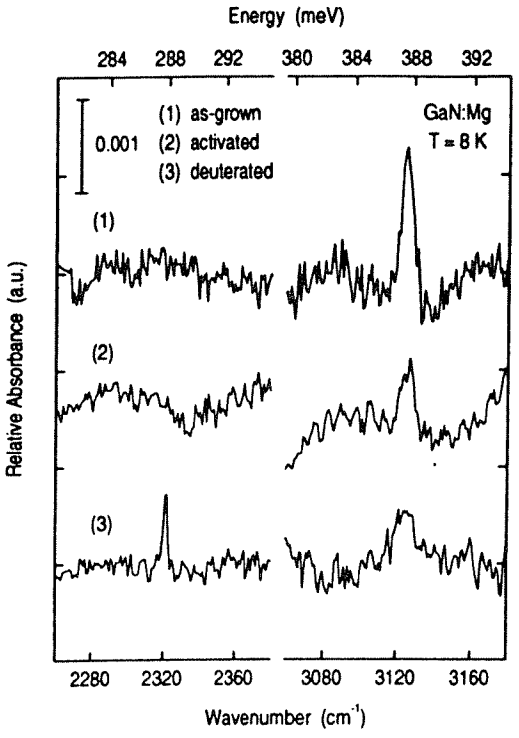

FIG. 7. Infrared absorption spectra for Mg-doped GaN grown by MOCVD. Spectra are shown for as-grown material (1), after RTA activation of the *p*-type conductivity (2), and after deuteration (3). The vertical bar indicates the magnitude of the absorbance scale. (Reprinted with permission from Götz *et al.*, 1996b.)

et al. (1994) in Mg-doped material cannot be associated with Mg—H complexes. As already pointed out by Brandt *et al.*, modes in this frequency range could be due to Ga—H bonds, for instance, at or near extended defects.

IV. Conclusions and Outlook

Most of our current knowledge about hydrogen interactions with nitrides comes from computational studies. Experimental work has established the main qualitative features, but quantitative assessments are lacking. As pointed out in Section III.5, the vibrational frequency of the Mg—H complex is currently the only reliably established physical parameter avail-

able from experiment. A major problem on the experimental side, of course, has been the lack of samples with sufficiently good crystal quality to perform reliable impurity studies. This problem will hopefully be addressed when bulk crystals, as well as material with lower defect densities, become available. The computational work has definitely pointed out some extremely interesting features that should be explored experimentally: for instance, the huge negative-U value for interstitial hydrogen in GaN.

The aspect of hydrogen that is best understood so far is its tendency to passivate acceptors, and the need to perform a post-growth treatment to activate the acceptors. Nonetheless, various aspects of the activation process need to be clarified. For instance, no conclusions have been reached regarding the mechanisms operative during the LEEBI treatment. Also, thermal annealing gives rise to interesting changes in the photoluminescence spectrum (see Götz *et al.*, 1996a) for which no explanation is available yet.

Only a few studies have been performed of the behavior of hydrogen on GaN surfaces, and its consequences for growth. Additional fundamental studies, both experimental and theoretical, would be very fruitful in this area and could potentially point the way toward improvements in the crystalline quality, suppression of defects, or incorporation of dopants.

The interaction between hydrogen and defects is just starting to be addressed. Regarding the native point defects, binding between hydrogen and vacancies is expected to occur and to play a role in the passivation (and potential activation upon annealing) of these defects. Computational work along these lines has recently been completed (Van de Walle, 1997), and experimental work on proton-implanted GaN has also been reported (Weinstein *et al.*, 1998). Of course, hydrogen may also interact with extended defects, such as dislocations.

Finally, we point out that almost all the work so far has focused on GaN, and few studies have been performed on hydrogen interactions with other nitrides (InN and AlN) or nitride alloys. Although qualitatively similar behavior is expected, the quantitative details could turn out to be very important. For instance, the role played by hydrogen in p-type doping of GaN (as discussed in Section III.4.b) could undergo some changes in AlGaN alloys; and, of course, doping of such alloy layers is essential for device structures. Studies of hydrogen in InGaN and AlGaN alloys are therefore necessary.

ACKNOWLEDGMENT

Thanks are due to W. Götz and J. Neugebauer for very productive collaborations.

REFERENCES

Akasaki, I., Amano, H., Kito, M., and Hiramatsu, K. (1991). *J. Lumin.*, **48&49**, 666.

Amano, H., Kito, M., Hiramatsu, K., and Akasaki, I. (1989). *Jpn. J. Appl. Phys.*, **28**, L2112.

Binari, S. C., Dietrich, H. B., Kelner, G., Rowland, L. B., Doverspike, K., and Wickenden, D. K. (1995). *J. Appl. Phys.*, **78**, 3008.

Boguslawski, P., Briggs, E. L., and Bernholc, J. (1995). *Phys. Rev. B*, **51**, 17255.

Bosin, A., Fiorentini, V., and Vanderbilt, D. (1996). *Mat. Res. Soc. Symp. Proc.*, **395**, Pittsburgh: Materials Research Society, p. 503.

Brandt, M. S., Ager, J. W. III, Götz, W., Johnson, N. M., Harris, J. S., Molnar, R. J., and Moustakas, T. D. (1994). *Phys. Rev. B*, **48**, 14758.

Chevallier, J., Clerjaud, B., and Pajot, B. (1991). In *Hydrogen in Semiconductors. Semiconductors and Semimetals*, **34**, J. I. Pankove and N. M. Johnson, eds. Boston: Academic Press, Chapter 13.

Chiang, C.-M., Gates, S. M., Bensaoula, A., and Schultz, J. A. (1995). *Chem. Phys. Lett.* **246**, 275.

Estreicher, S. K. (1994). In *Hydrogen in Compound Semiconductors.* S. J. Pearton, ed., Mat. Sci. Forum, **148–149**, p. 349. Aedermannsdorf: Trans Tech.

Estreicher, S. K. (1995). *Mat. Sci. Engr. Reports*, **14**, 319.

Estreicher, S. K. and Maric, D. M. (1996). *Mat. Res. Soc. Symp. Proc.* **423**, Pittsburgh: Materials Research Society, p. 613.

Götz, W., Johnson, N. M., Walker, J., Bour, D. P., Amano, H., and Akasaki, I. (1995). *Appl. Phys. Lett.*, **67**, 2666.

Götz, W., Johnson, N. M., Walker, J., Bour, D. P., and Street, R. A. (1996a). *Appl. Phys. Lett.*, **68**, 667.

Götz, W., Johnson, N. M., Bour, D. P., McCluskey, M. D., and Haller, E. E. (1996b). *Appl. Phys. Lett.*, **69**, 3725.

Götz, W. and Johnson, N. M. (1997). Unpublished.

Hamann, D. R., Schlüter, M., and Chiang, C. (1979). *Phys. Rev. Lett.*, **43**, 1494.

Hohenberg, P. and Kohn, W. (1964). *Phys. Rev.*, **136**, B864.

Johnson, B. G., Gill, P. M. W., and Pople, J. A. (1993). *J. Chem. Phys.*, **98**, 5612.

Johnson, N. M., Herring, C., and Van de Walle, C. G. (1994). *Phys. Rev. Lett.*, **73**, 130.

Kohn, W. and Sham, L. J. (1965). *Phys. Rev.*, **140**, A1133.

Laks, D. B., Van de Walle, C. G., Neumark, G. F., and Pantelides, S. T. (1991). *Phys. Rev. Lett.*, **66**, 648.

Lee, J. W., Pearton, S. J., Zolper, J. C., and Stall, R. A. (1996). *Appl. Phys. Lett.*, **68**, 2102.

Li, X. and Coleman, J. J. (1996). *Appl. Phys. Lett.*, **69**, 1605.

Louie, S. G., Froyen, S., and Cohen, M. L. (1982). *Phys. Rev. B*, **26**, 1739.

Nakamura, S., Iwasa, N., Senoh, M., and Mukai, T. (1992). *Jpn. J. Appl. Phys.*, **31**, 1258.

Neugebauer, J. and Van de Walle, C. G. (1994a). *Mat. Res. Soc. Symp. Proc.*, **339**, Pittsburgh: Materials Research Society, p. 687.

Neugebauer, J. and Van de Walle, C. G. (1994b). *Phys. Rev. B*, **50**, 8067.

Neugebauer, J. and Van de Walle, C. G. (1995a). *Phys. Rev. Lett.*, **75**, 4452.

Neugebauer, J. and Van de Walle, C. G. (1995b). *Mat. Res. Soc. Symp. Proc.*, **378**, Pittsburgh: Materials Research Society, p. 503.

Neugebauer, J. and Van de Walle, C. G. (1996a). *Appl. Phys. Lett.*, **68**, 1829.

Neugebauer, J. and Van de Walle, C. G. (1996b). *Mat. Res. Soc. Symp. Proc.*, **423**, Pittsburgh: Materials Research Society, p. 619.

Ohba, Y. and Hatano, A. (1994). *Jpn. J. Appl. Phys.*, **33**, L1367.

Okamoto, Y., Saito, M., and Oshiyama, A. (1996). *Jpn. J. Appl. Phys.*, **35**, L807.

Pankove, J. I. and Johnson, N. M., eds. (1991). *Hydrogen in Semiconductors. Semiconductors and Semimetals*, **34**, R. K. Willardson and A. C. Beer, Treatise eds. Boston: Academic Press.

Pavesi, L. and Giannozzi, P. (1992). *Phys. Rev. B*, **46**, 4621.

Pearton, S. J., Corbett, J. W., and Stavola, M. (1992). *Hydrogen in Crystalline Semiconductors*. Berlin: Springer-Verlag.

Pearton, S. J., Shul, R. J., Wilson, R. G., Ren, F., Zavada, J. M., Abernathy, C. R., Vartuli, C. B., Lee, J. W., Mileham, J. R., and Mackenzie, J. D. (1996a). *J. Electron. Mat.*, **25**, 845.

Pearton, S. J., Abernathy, C. R., Vartuli, C. B., Lee, J. W., Mackenzie, J. D., Wilson, R. G., Shul, R. J., Ren, F., and Zavada, J. M. (1996b). *J. Vac. Sci. Technol. A*, **14**, 831.

Pearton, S. J., Lee, J. W., and Yuan, C. (1996c). *Appl. Phys. Lett.*, **68**, 2690.

Pearton, S. J., Bendi, S., Jones, K. S., Krishnamoorthy, V., Wilson, R. G., Ren, F., Karlicek, R. F., Jr., and Stall, R. A. (1996d). *Appl. Phys. Lett.*, **69**, 1879.

Stavola, M. and Pearton, S. J. (1991). In *Hydrogen in Semiconductors, Semiconductors and Semimetals*, **34**, J. I. Pankove and N. M. Johnson, eds. Boston: Academic Press, Chapter 8.

Sung, M. M., Ahn, J., Bykov, V., Rabalais, J. W., Koleske, D. D., and Wickenden, A. E. (1996). *Phys. Rev. B*, **54**, 14 652.

Van de Walle, C. G., Denteneer, P. J. H., Bar-Yam, Y., and Pantelides, S. T. (1989). *Phys. Rev. B*, **39**, 10791.

Van de Walle, C. G., Laks, D. B., Neumark, G. F., and Pantelides, S. T. (1993). *Phys. Rev. B*, **47**, 9425.

Van de Walle, C. G. and Neugebauer, J. (1997). *Mat. Res. Soc. Symp. Proc.*, **449**, Pittsburgh: Materials Research Society, p. 861.

Van de Walle, C. G. (1997). *Phys. Rev. B*, **56**, R10 020.

Van Vechten, J. A., Zook, J. D., Horning, R. D., and Goldenberg, B. (1992). *Jpn. J. Appl. Phys.*, **31**, 3662.

Weinstein, M. G., Song, C. Y., Stavola, M., Pearton, S. J., Wilson, R. G., Shul, R. J., Killeen, K. P., and Ludowise, M. J. (1998). *Appl. Phys. Lett.*, **72**, 1703.

Wilson, R. G., Pearton, S. J., Abernathy, C. R., and Zavada, J. M. (1995). *J. Vac. Sci. Technol. A*, **13**, 719.

Yu, Z., Buczkowski, S. L., Giles, N. C., Myers, T. H., and Richards-Babb, M. R. (1996). *Appl. Phys. Lett.*, **69**, 2731.

Zavada, J. M., Wilson, R. G., Abernathy, C. R., and Pearton, S. J. (1994). *Appl. Phys. Lett.*, **64**, 2724.